Investigating Applicability of Surface Roughness Parameters in Describing the Metallic AM Process

Samantha Taylor[1,2], Bradley Jared[1], Josh Koepke[1], Eric Forrest[1], Joseph Beaman[2]

[1]Sandia National Laboratories, Albuquerque, NM 87123

[2]Department of Mechanical Engineering, The University of Texas at Austin, Austin, TX 78705

Abstract

Additive manufacturing (AM) is known for its large variance in mechanical properties. This is not only true for properties like strength, but also surface roughness. Build settings, which affect surface roughness, are often chosen to optimize strength or ductility. As part requirements change, build settings change, thereby changing resultant surface roughness. When describing surfaces, arithmetic roughness (R_a) is the most common parameter. However, it may not provide an adequate representation of surface topography for AM parts. Traditional surface roughness parameters for defining surface topography were well-established before the advent of AM, and a need has arisen to investigate applicability of these parameters to the unusual surfaces created through various AM technologies. This study demonstrates that R_a is not a suitable parameter in correlating surface topography to AM build parameters. Other existing parameters and combination of parameters will be investigated for their suitability in describing the AM process.

Background

Additive manufacturing (AM) is becoming increasingly popular for a variety of applications. Since AM is unique in that both the dimensional shape and material properties are being formed at the same time, traditional qualifications methods need to be updated. To qualify a part using non-destructive methods means leveraging every possible measurement to indicate the material quality of the part. One such measurement is surface roughness. Surface roughness has always been a dictated part requirement, which is still the case, but now it is also being used as an indicator of the AM process. Especially in metallic AM process, such as laser powder bed fusion (L-PBF), surface roughness can be an indication of the process, which will be discussed in later sections. This paper will investigate the applicability of using surface topography as an indication of the AM process quality. The focus will specifically be on metallic parts created with the L-PBF process as it the most popular of the metallic AM technologies and therefore has had the most research performed related to it [1]. The material of focus for this study will be 316 stainless steel as it is popular in industry and has also been the largest focus of the of metallic AM surface roughness research [1].

Surface Roughness Standards

ASME B46.1 [2] and ISO 4287 [3] are the two commonly used standards for defining surface texture, including roughness, waviness, and lay. In both standards, techniques for measuring, analyzing, and defining surface topography are present. Within both standards, universal surface roughness parameters are defined. The most common of these parameters is average roughness, R_a, which relates to the mean height of the surface. The equation used for

calculation can be found in Equation 2. A representative surface with definitions can be found in Figure 1.
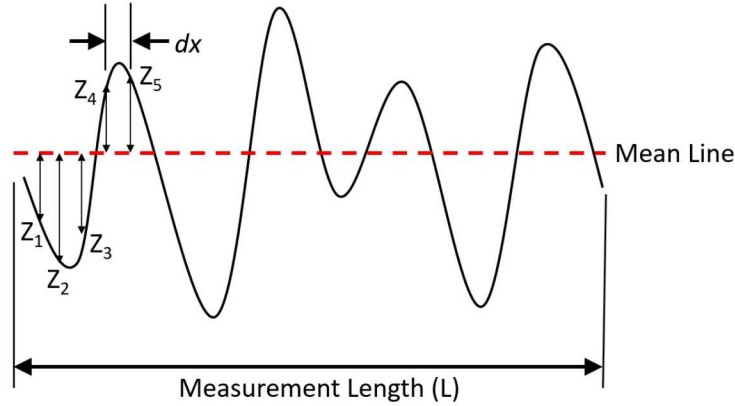

Figure 1: Surface Roughness Variables Diagram.

$$R_a = \frac{1}{L} \int_0^L |Z(x)| dx \tag{1}$$

Other common surface roughness parameters include root mean square roughness (R_q), skewness (R_{sk}), and kurtosis (R_{ku}). The respective equations for each can be found in Equations 2-4. Skewness is a numerical indication of the surface's presence about the calculated mean line. A negative value for skewness represents a surface mainly composed of valleys, while a positive valued surface is mainly composed of peaks. Kurtosis is the measure of the sharpness of the peaks of the surface. The creation of these standard surface roughness definitions preceded the advent of additive manufacturing. Therefore, it is important to ascertain their effectiveness in not only delineating different AM surfaces but also in correlating topography to AM process settings. One such parameter that was suggested in Grimm et al. as a more effective delineator was $R\Delta q$, or root mean square slope [4]. The equation for this parameter can be found in Equation 5. $R\Delta q$ is a unitless parameter whose value as it increases indicates steeper slopes in the surface topography.

$$R_q = \sqrt{\frac{1}{L} \int_0^L Z(x)^2 dx} \tag{2}$$

$$R_{sk} = \frac{1}{R_q{}^3} \frac{1}{L} \int_0^L Z^3(x) dx \tag{3}$$

$$R_{ku} = \frac{1}{R_q{}^4} \frac{1}{L} \int_0^L Z^4(x) dx \tag{4}$$

2

$$R\Delta q = \sqrt{\frac{1}{L}\int_0^L \left(\frac{dZ}{dx}\right)^2 dx} \tag{5}$$

The standards not only define linear surface roughness parameters, but also area parameters as well. Most linear surface roughness parameters can be translated into area parameters by measuring in two perpendicular directions. Examples of the area parameter for average roughness and root mean square slope can be found in Equations 6 and 7 below.

$$S_a = \frac{1}{A}\int_0^{L_y}\int_0^{L_x} |Z(x,y)| dxdy \tag{6}$$

$$S\Delta q = \sqrt{\frac{1}{A}\int_0^{L_y}\int_0^{L_x} \left(\frac{dZ(x,y)}{dx}\right)^2 + \left(\frac{dZ(x,y)}{dy}\right)^2 dxdy} \tag{7}$$

Surface Roughness in Additive Manufacturing

Additive manufacturing has created unique surface finishes that range in both size and feature types depending on the process used. Processes like laser engineered net shaping (LENS) and laser powder bed fusion (L-PBF), can create surfaces rougher than those generated with traditional subtractive manufacturing techniques. For example, stainless steel surfaces that were finished with conventional milling practices have R_a values of roughly 1-4 microns and $R\Delta q$ values less than 0.5. These values were measured with parts that were produced during this study as a roughness comparison to the AM parts. In traditional manufacturing, surface roughness is instructive for how smooth or rough the surface of a part needs to be for its intended purpose. Whereas in additive manufacturing, surface roughness for the end use part can be specified, but researchers are also using it as an indicator of the process, the purpose of this study.

Due to the popularity of laser powder bed fusion processes such as L-PBF over other metal additive techniques such as electron beam additive manufacturing (EBAM), this category of additive manufacturing will be the focus of this study. A sample of a L-PBF generated top surface can be found in Figure 2.
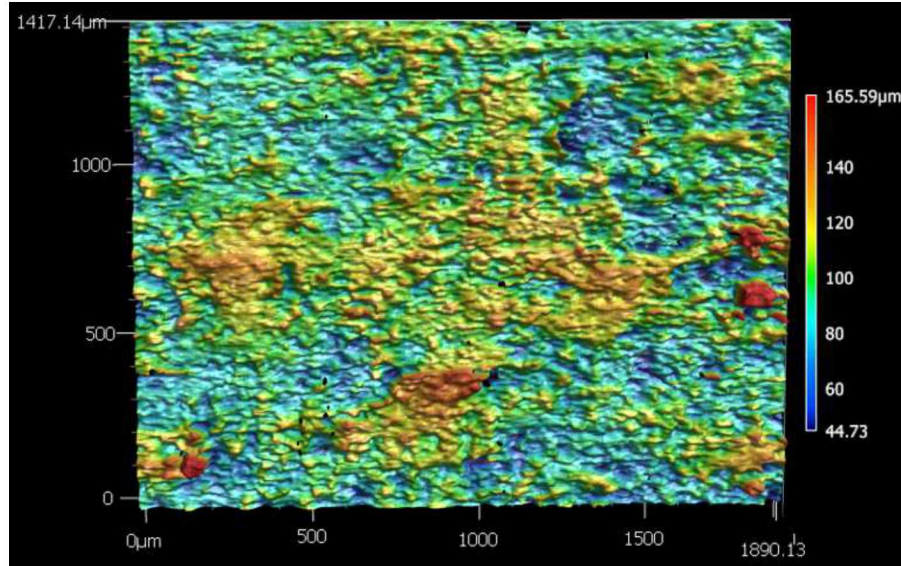
Figure 2: 160x Magnification Surface Height Map of 316 Stainless Steel AM Part created with L-PBF.

In metallic laser powder bed fusion, there are two main ways surface roughness is generated on the horizontal or top surface. The first major phenomenon is the solidification of ripples generated in the melt pool as the laser moves across the powder bed. These ripples are caused by shear forces generated through thermal gradient present in the process. Since the process is moving at high speeds and the solidification time for metals is short, the ripples become frozen, generating surface roughness [5]. This effect can be seen in Figure 3, which is a scanning electron microscope (SEM) image of a stainless steel surface generated with the L-PBF process. Scan tracks are clearly visible with ripples contained in them.
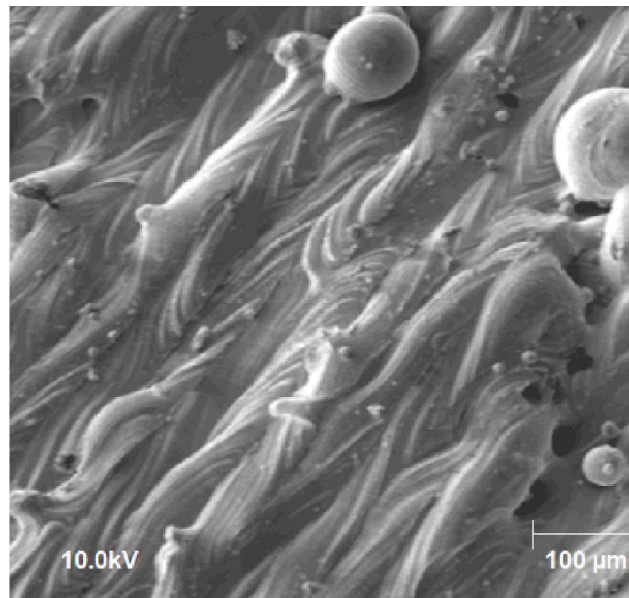

Figure 3: SEM Image of Stainless Steel L-PBF Sample Top Surface with Rippling and Balling Effects.

The other major phenomenon that creates rough surface features is balling. This can be generated when the laser power is too high, causing material to be ejected from the melt pool

4

which solidifies on other parts of the surface [6]. This phenomena can be seen in Figure 3 in addition to a 3D height map taken of a surface shown in Figure 4 where some of the solidified ejected material is circled.
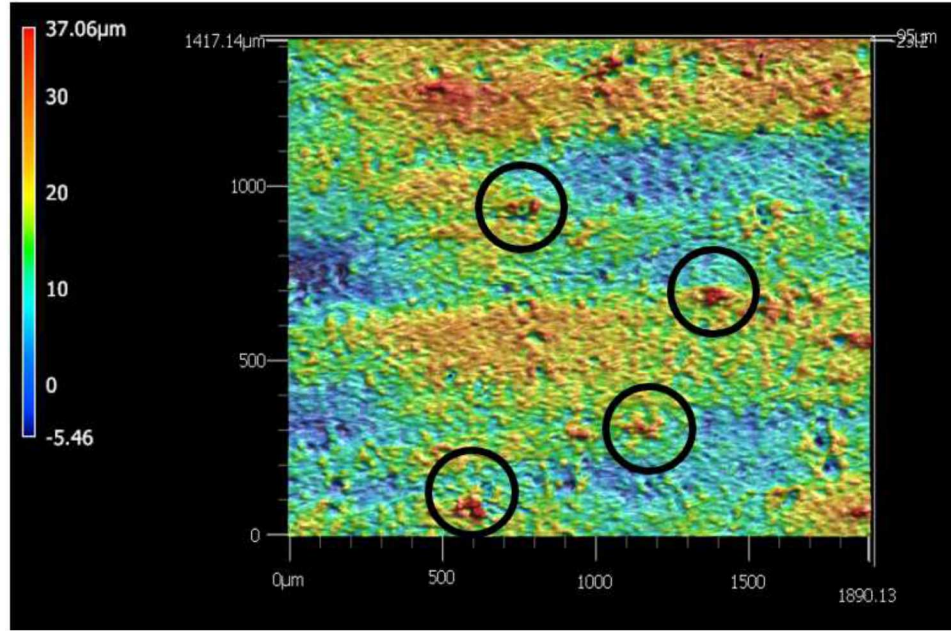

Figure 4: 3D Height Map of L-PBF Surface with Instances of Balled Material Circled.

For all angled surfaces of the part, the major contributing factors for surface roughness are partially melted powder and stair stepping, which results from the layer-wise build process found in most additive techniques. Since almost all lasers used in metal powder bed fusion processes are a Gaussian beam, the edges of the beam partially melt powder on the edges of the part due to a lack of power [5].

Since the surface texture of horizontal surfaces is highly dependent on the melt pool dynamics, certain process parameters have a considerable influence on the surface roughness. Rombouts et al. found that scan speed and scan spacing, which is the distance between the centerline of successive scan lines, to be the most influential process parameters on surface roughness [7]. As seen in the literature, there are a wide range of parameters used in both research and industry. The scanning parameters of speed, scan spacing, and laser power are chosen based on both material and whatever final part properties the manufacturer determines as paramount. Most research focuses on mechanical properties, for which the process parameters will be tuned for optimization. Therefore, the parameters that are chosen can have a broad range, which would result in numerous possible surface textures.

Experimental Procedure

To demonstrate the range of surfaces produced by the laser powder bed fusion process, a range of process parameters was used to produce the samples. The key value in the L-PBF process that many researchers control to change the quality of parts is the energy density input into powder bed. The equation for applied energy density is seen below in Equation 8 [8].

$$E_A = \frac{Laser\ Power}{Scan\ Velocity \times Scan\ Spacing} \qquad (8)$$

Another commonly used descriptor for the additive process, is volumetric energy density (VED). This parameter is nearly the same to the applied energy density with the exception that layer thickness is also in the denominator of the equation. VED describes the amount of energy input into a volume of material during the L-PBF process. Although only one parameter change is needed to affect the energy density, two variables were altered throughout the building process to affect the other mechanisms at play that affect surface topography, density, and mechanical strength such as heat transfer and fluid dynamics seen in the melt pool. As was stated in introduction section, the generation of surface roughness is directly related to both laser power and scan speed. Therefore, laser power and scan speed were the only variables that were changed for this specific study. Scan spacing was not varied for these parts as the focus was on the effects of laser power and scan speed.

The parts were built on a 3D Systems ProX 200. Parts were built with laser powers ranging from 20-180 Watts, and scan speeds ranging from 300 to 2000 mm/s. The parts built were 1 cm cubes. The cube design was chosen so that surface roughness and part density could be measured. Most parts were built in sets of 24 on a single build plate. Some were built with only 10 cubes per build plate. A sample image of the completed build with 21 out of 24 cubes moving on for measurement can be found in Figure 5. As seen in the figure, there is one cube that delaminated early on in the first column on the left and two cubes which also had issues located at the top of the second column from the left and the fourth cube down from the third column from the left.

Figure 5: Sample Cube Build Plate [9].

Most of the parts were built with 316L stainless steel powder with a mean particle size of 15 microns. The layer thickness for most parts was 30 microns, but there were two builds that had 40 micron layer thickness. For certain combinations of parameters, the cubes were not completed due to a lack of fusion or extremely rough surfaces that did not allow the powder roller of the machine to proceed in placing an even layer of powder down. These combinations had either too low or too high energy density. For example, very slow scan speeds with high laser power produced parts that were too rough for the process to continue due to over-melting

and part distortion. Therefore, the data presented is only the subset of parameters that allowed the cubes to be fully built. A total of 80 parts were able to be fully completed. Further details for the build procedures and on which settings were used when parts failed can be found in Koepke et al. [9].

Part density was measured using the Archimedes method which uses the volume of liquid displaced by an object to calculate mass and volume of said object. For surface roughness measurements, there are two problems with metallic AM parts. The first is the highly reflective nature of the parts, which interferes with some of the non-contact techniques used to measure surface roughness. The second issue is the highly rough and irregular nature of the surfaces produced, which can affect both non-contact and contact techniques. These issues prevent focus variation microscopy and white light interferometry from being used to measure the surfaces accurately [1]. Contact profilometry was considered, but due to its slow speed and risk of damaging the equipment with the rough AM surfaces, it was not used. Fringe pattern projection microscopy was the measurement technique used to measure the surface roughness of the as built AM samples. This method projects fringe patterns with variable frequency and position onto the sample. Using a CMOS sensor which detects the fringe pattern distortions and computer algorithms, it calculates the surface heights of an area of interest. A diagram of this function can be seen in Figure 6 below. The specific measurement device used was a Keyence VR3100 visual macroscope.
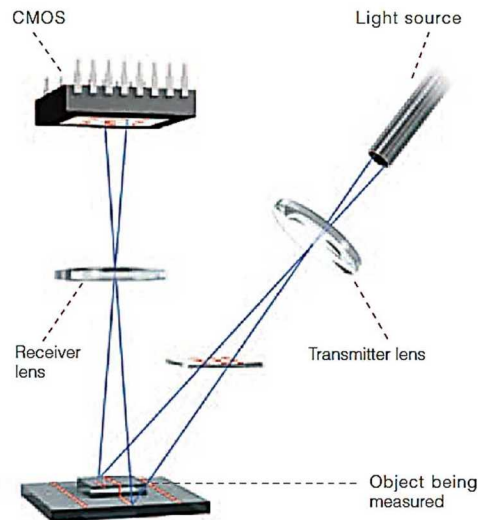

Figure 6: Keyence VR3100 Visual Macroscope Functional Diagram [10].

The dimensions of the area that is measured depends on the focus selected at the time of measurement. At the lowest magnification, 12x, the area measured is about 24 × 18 mm. At the highest magnification, 160x, the area measured is about 1.9 × 1.4 mm with a height resolution of 0.1 μm [10]. Examples of the height map produced from each magnification can be seen in
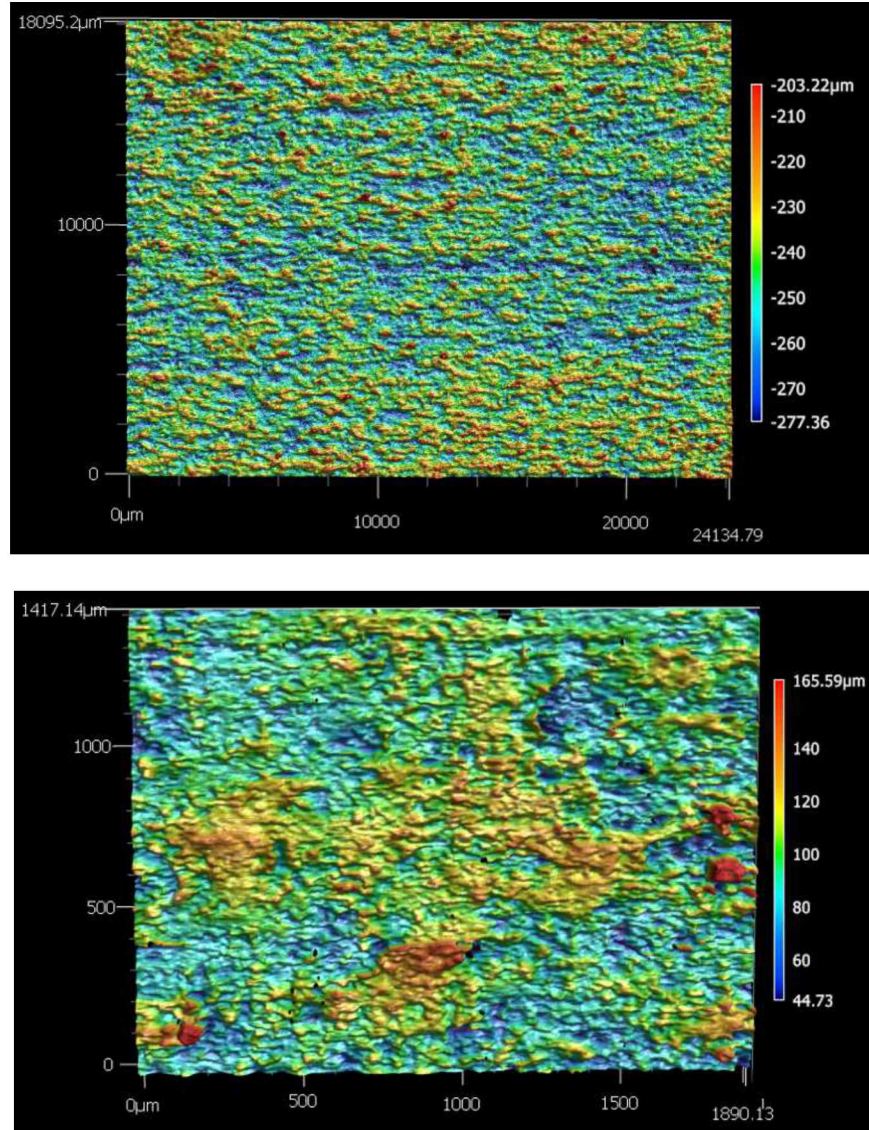
Figure 7.

Figure 7: (TOP): 12x Magnification 3D Height Map of L-PBF Sample **(BOTTOM):** 160x Magnification 3D Height Map of L-PBF Sample.

The highest magnification was used for all surface parameter calculations. The associated Keyence software that views and processes all the macroscope data calculated the surface roughness parameters that were used for this analysis.

Results

Various surface roughness parameters were plotted against volumetric energy density and part density to observe the correlation strengths between them. The coefficient of determination, or R^2 value, is an indication of how well the predictive model data fits with the existing data. The same type of trend line, a power function, was used across all parameters for ease of comparison. The arithmetic mean height has been the most common surface roughness parameter in AM literature when describing surface roughness [1]. Therefore, it was included in the analysis below to observe its correlation strength. The relationships to density and VED for arithmetic

mean height (S_a) and Kurtosis (S_{ku}), which is another commonly used surface roughness parameter in traditional manufacturing, can be found in Figures 7-10. As can be seen in Figure 8 and Figure 9, S_a is insufficient for indicating differences in volumetric energy density and part density. Since S_a only gives an average number for the height, there can be different shapes between surfaces with the same S_a value. The shapes of these surfaces alter with the volumetric energy density and may influence the part density since powder settling for each layer can be affected by the previous layer's shape.
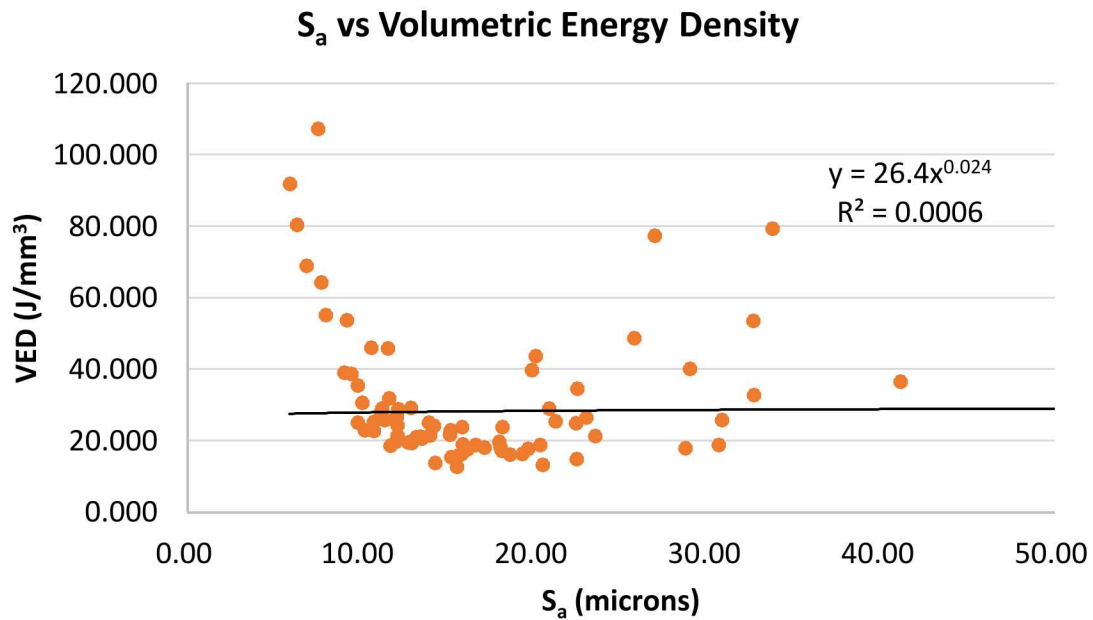
S_a vs Volumetric Energy Density

$$y = 26.4x^{0.024}$$
$$R^2 = 0.0006$$

Figure 8 plots VED (J/mm³) on the vertical axis against S_a (microns) on the horizontal axis.

Figure 8: Arithmetic Mean Height Plotted Against Volumetric Energy Density.

S_a vs Density
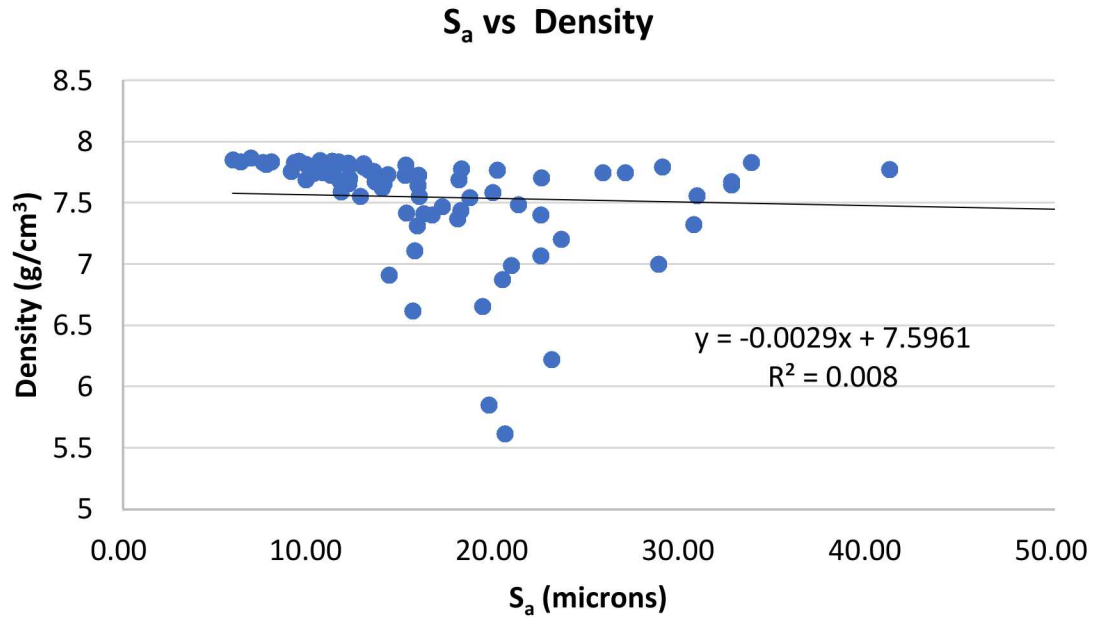

$$y = -0.0029x + 7.5961$$
$$R^2 = 0.008$$

Figure 9: Arithmetic Mean Height Plotted Against Part Density.

Kurtosis, which does indicate the shape of the peaks of a surface is also insufficient in indicating differences between VED and part density. This parameter does indicate certain aspects of the surface's shape but is insufficient for fully describing the varying surfaces caused by different build settings.
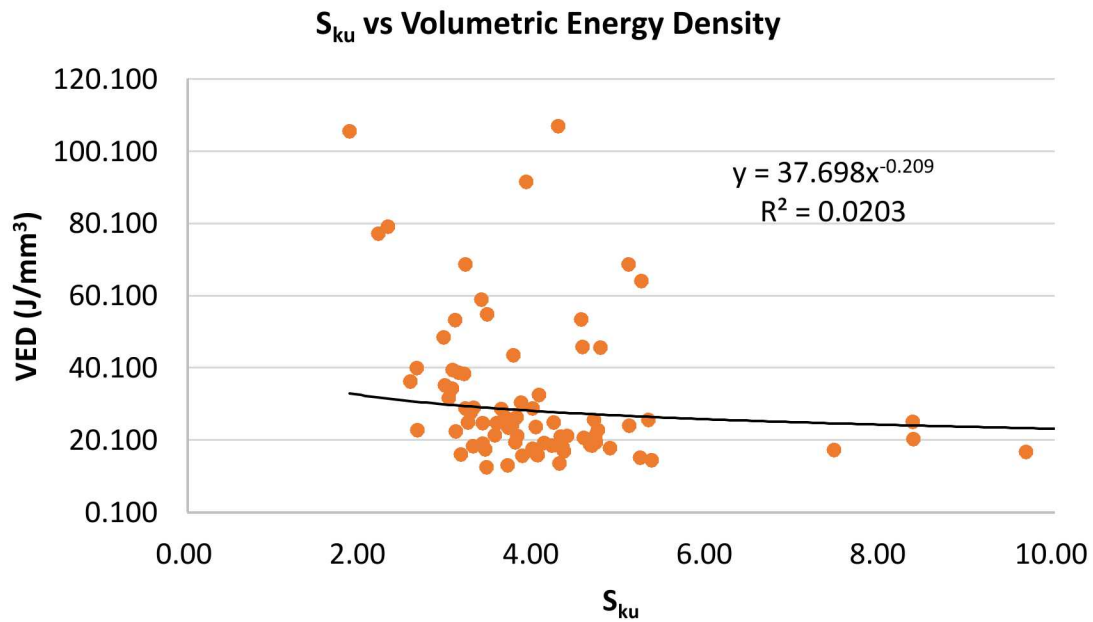
S_{ku} vs Volumetric Energy Density

$$y = 37.698x^{-0.209}$$
$$R^2 = 0.0203$$

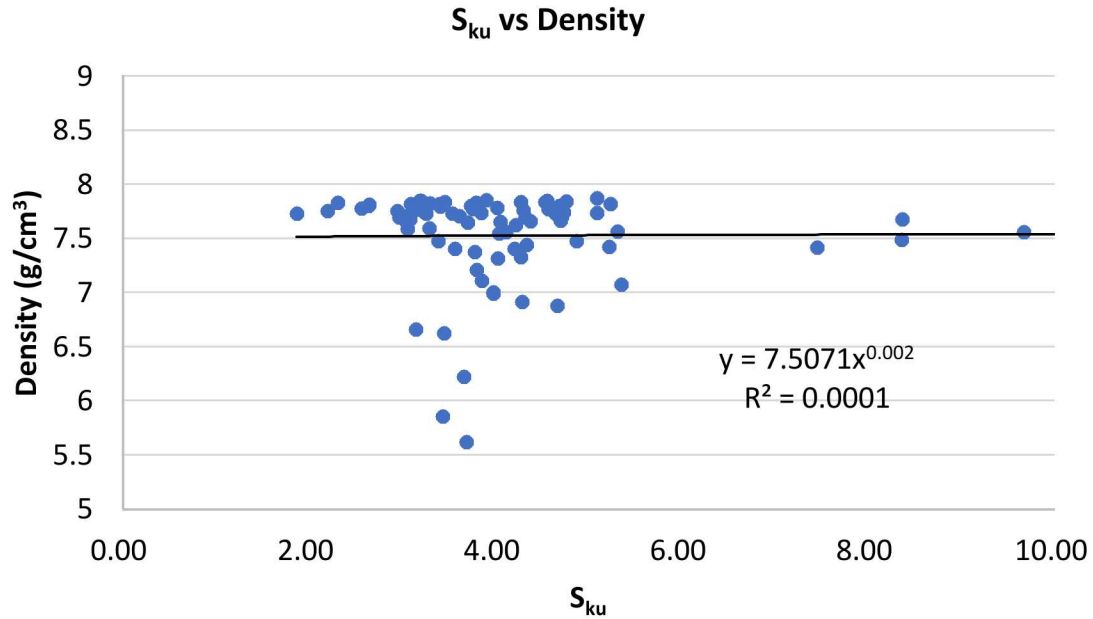**Figure 10:** Kurtosis Plotted Against Volumetric Energy Density.

Figure 11: Kurtosis Plotted Against Part Density.

When looking at the less common surface parameters from the existing standards, their correlation levels improve. Root mean square slope ($S\varDelta q$) had the highest correlation to both VED and part density. This parameter describes the slope of the surface, which is directly tied to the process parameters that are used to calculated VED.
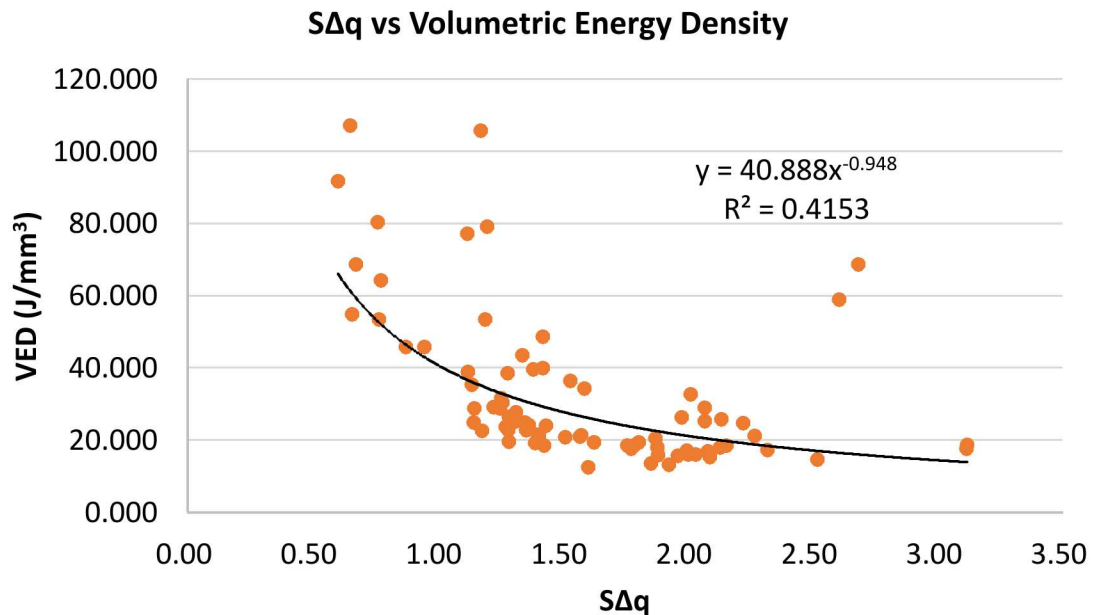

Figure 12: Root Mean Square Slope Plotted Against Volumetric Energy Density.
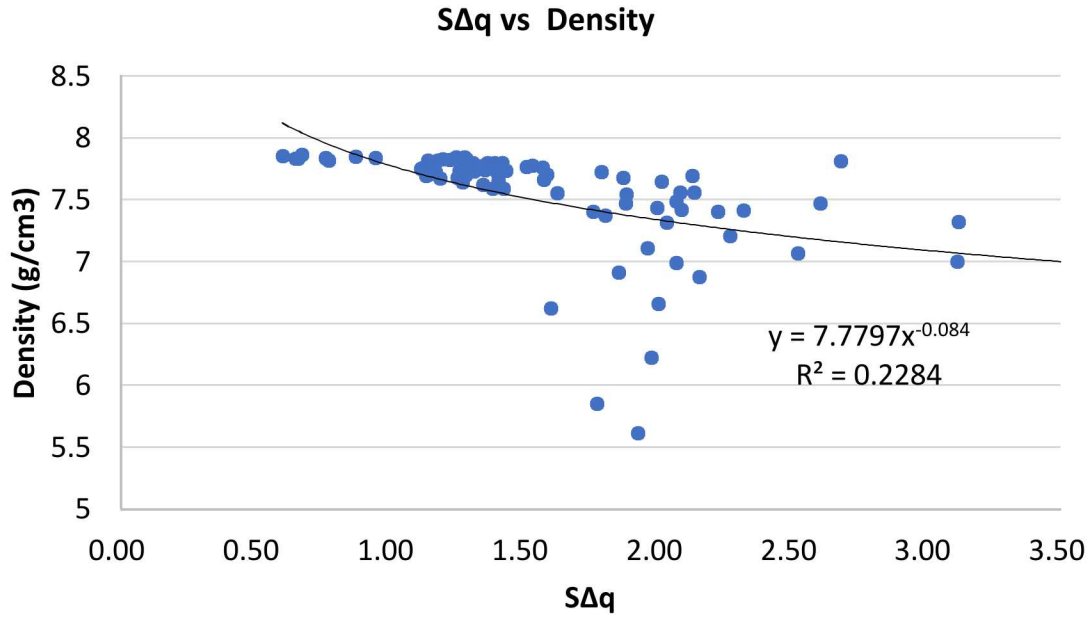
SΔq vs Density

Figure 13: Root Mean Square Slope Plotted Against Part Density.

Another less commonly used parameter termed peak density (S_{pd}) was tested during this experimental study. Peak density counts the number of peaks of the surface for a given area. It had higher correlation to VED than S_a or S_{ku} but had the same level of correlation for density. It's clear that as the VED is an indication of the possible dynamics of the process, that the peak density would be affected since those peaks are generated by the frozen ripples formed during the process. However, peak density does not indicate the varying heights of the peaks, and therefore does not relate as well to density as the root mean square slope.
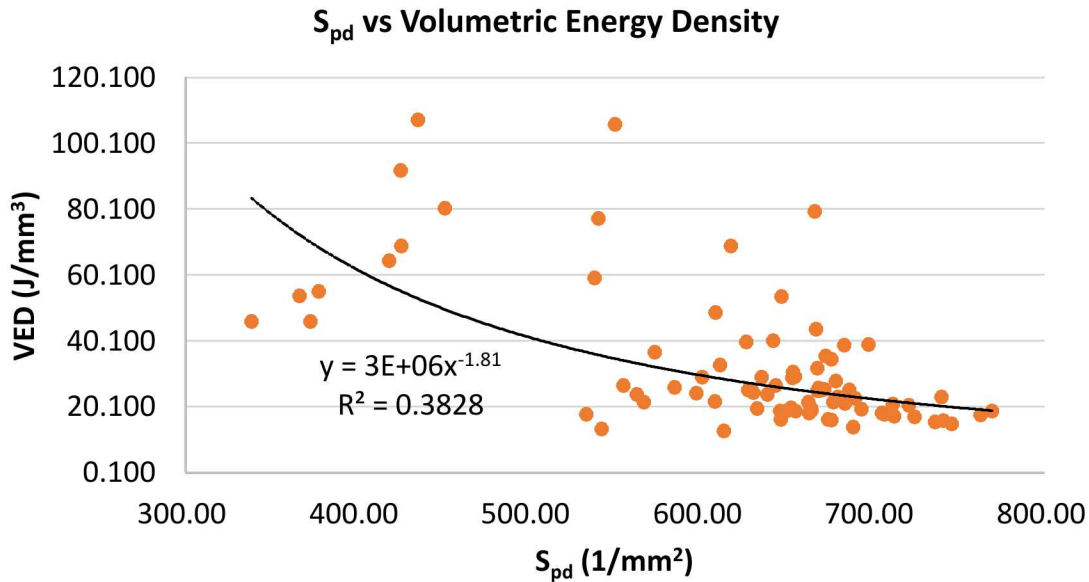

S_{pd} vs Volumetric Energy Density

Figure 14: Peak Density Plotted Against Volumetric Energy Density.

12

S_{pd} vs Density

The chart shows a scatter plot with a fitted trend line. The axis labels are Density (g/cm³) on the vertical axis (ranging from 5 to 9) and S_{pd} (1/mm²) on the horizontal axis (ranging from 300.00 to 800.00). The fitted equation shown is:
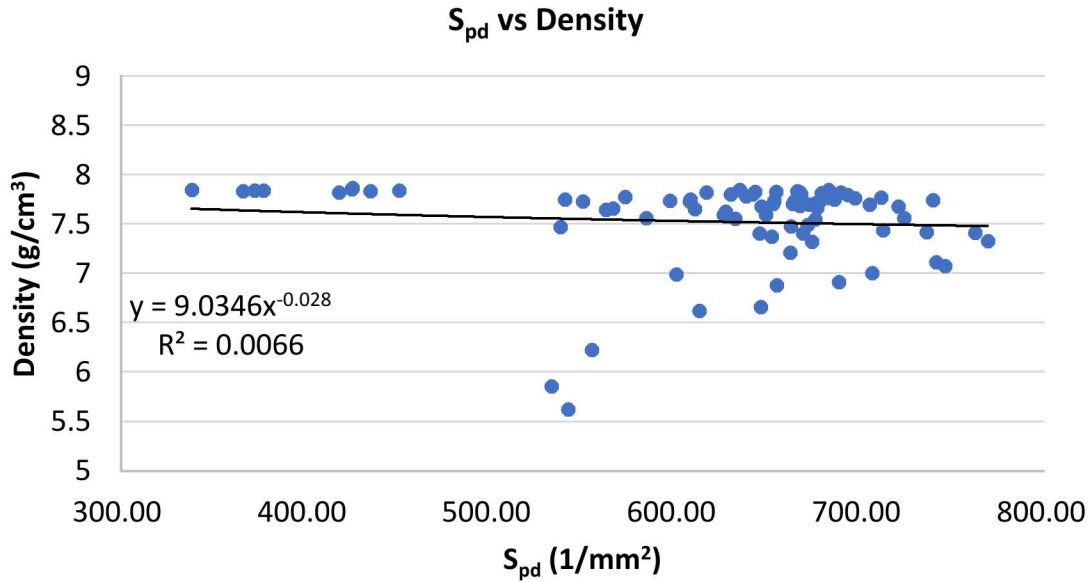
$$y = 9.0346x^{-0.028}$$
$$R^2 = 0.0066$$

Figure 15: Peak Density Plotted Against Part Density.

Conclusions

As seen through the comparison of several surface roughness parameters, not all current parameters are suited for describing the additive manufacturing process. Arithmetic mean height (S_a) is not suited for delineating between different additive parts, even though it is currently the most popular parameter when discussing surface roughness in AM literature. Root mean square slope ($S\Delta q$) is a better delineator as it seems to better indicate the surface topography features that are generated and changed when changing volumetric energy density input into a metallic L-PBF part. However, more investigation is required to find the best existing surface roughness parameter. This work highlights the need for improved surface roughness standards, parameters, and measurement techniques to better describe parts produced through AM processes.

Acknowledgements

References

[1] A. Townsend, N. Senin, L. Blunt, R. K. Leach and J. S. Taylor, "Surface Texture Metrology for Metal Additive Manufacturing: A Review," *Precision Engineering,* no. 46, pp. 34-47, 2016.

[2] ASME, *B46.1: Surface Texture (Surface Roughness, Waviness, and Lay),* 2009.

[3] International Organization for Standardization, *Geometric Product Specifications (GPS) - Surface Texture: Profile Method - Terms, Definitions, and Surface Texture Parameters,* Geneva, 1997.

[4] T. Grimm, G. Wiora and G. Witt, "Characterization of Typical Surace Effects in Adiditve Manufacutring with confocal Microscopy," *Surface Topogrphy: Metrology and Properties,* no. 3, pp. 1-12, 2015.

[5] G. Strano, L. Hao, R. Everson and K. Evans, "Surface Roughness Analysis, Modelling, and Predition in Selective Laser Melting," *Journal of Materials Processing Technology,* no. 213, pp. 589-597, 2012.

[6] Y. Tian, D. Tomus, P. Rometsch and X. Wu, "Influence of Processing Parameters on Surface Roughness of Hastelloy X Produced by Selective Laser Melting," *Additive Manufacturing,* pp. 103-112, 2017.

[7] M. Rombouts, G. MAes, W. Hendrix, E. Delarbre and F. Motmans, "Surface Finish After Laser Metal Deposition," *Physics Procedia,* no. 41, pp. 810-814, 2013.

[8] I. Gibson, D. Rosen and B. Stucker, Additive Manufacturing Technologies: 3D PRinting, Rapid Prototyping, and Direct Digital Manufacturing, New York: Springer, 2015.

[9] J. R. Koepke, B. Jared and Y.-L. Shen, "The Influence of Process Variables on Physical and Mechanical Properties in Laser Powder Bed Manufacturing," 2019. [Online]. Available: https://digitalrepository.unm.edu/me_etds/164 . [Accessed 2019].

[10] Keyence Corporation, "VR-3100 - Wide-Area 3D Measurement System Sensor Head," 2018. [Online]. Available: https://www.keyence.com. [Accessed 25 May 2018].

[11] Keyence Corporation, "Area Roughness Parameters," 2019. [Online]. Available: https://www.keyence.com/ss/products/microscope/roughness/surface/sdq-root-mean-square-gradient.jsp. [Accessed 31 January 2019].

[12] S. Kleszczynski, A. Ladewig, K. Friedberger, J. zur Jacobsmuhlen, D. Merhof and G. Witt, "Position Dependency of Surface Roughness in Parts from Laser Beam Melting Systems," in *Solid Freeform Fabrication Symposium*, Austin, 2015.

[13] J. C. Fox, S. P. Moylan and B. M. Lane, 30 June 2016. [Online]. Available: www.nist.gov. [Accessed February 2018].